

INTRODUCTION

During an earthquake, the potential energy is transferred to elastic wave energy and non-radiated energy, E_R and E_{NR} , respectively. The non-radiated energy is here composed by E_G and E_H , where E_G is the fracture energy required to mechanically weaken the fault, and E_H the energy dissipated locally by frictional heating around the fault (Kanamori & Heaton, 2000). Considering this, the energy budget during a rupture propagation corresponds to the sum of E_R , E_G and E_H (Knopoff, 1958).

The stress drops from the initial to the final stress (σ_0 to σ_1), corresponds to before and after the earthquake. $\Delta\sigma_s$ represents this difference, and it is called static stress-drop (Figure 1). On the same way, during sliding, the stress is equal to the frictional stress, σ_f , which in general is varying during faulting. However, in the simplest model the frictional stress is constant, defined as the average of the frictional stress during the motion (Kanamori, 2001).

In this research, the temperature increases produced by local events were estimated. These results allowed us to calculate the maximum total amount of thermal energy produced by the local seismicity recorded in southern Norway in the period 2017-2018. For this, a simple stress release model was used, which avoids considering stress variations during the motion. As a second step, these results were utilized to develop a comprehensive study about the relationship and correlations between the behavior of local seismicity with the effects of heating and cumulative energy.

METHODOLOGY

The temperature rise was calculated by considering the gross thermal budget during faulting under a constant frictional stress σ_f , as shown in Figure 1 (Kanamori & Heaton, 2000). Defining S and D as the fault area and the displacement offset, respectively, the total heat, Q , generated during faulting could be obtained by (1).

$$Q = \sigma_f DS$$

If the heat is distributed during seismic faulting within a layer of thickness w (0.1 - 1 cm; Kanamori & Heaton, 2000) around the rupture plane, then the average temperature rise could be expressed by (2), where C is the specific heat (1 J/g°C) and ρ is the density (2.6 g/cm³).

$$\Delta T = \frac{Q}{C\rho Sw} = \frac{\sigma_f D}{C\rho w}$$

Using a simple circular model (Eshelby, 1957; Kanamori & Heaton, 2000) in which the static stress drop is $\Delta\sigma_s$, μ is the rigidity (0.3 Mbar) and M_0 is the seismic moment, it is possible to write the displacement offset, D , as (3).

$$D = \left(\frac{16}{7}\right)^{2/3} \frac{1}{\pi\mu} \sigma_f \Delta\sigma_s^{2/3} M_0^{1/3}$$

$$\Delta T = \left(\frac{16}{7}\right)^{2/3} \frac{1}{\pi\mu C\rho w} \sigma_f \Delta\sigma_s^{2/3} M_0^{1/3}$$

By combining equations (2) and (3), the temperature rise was defined by (4).

$$\log M_0 = 1.5M_w + 9.1$$

The seismic moment is related to M_w through (5).

$$M_w = \frac{2}{3} M_L + 1.15$$

The conversion of local (M_L) to moment (M_w) magnitudes for small earthquakes was proposed by Munafo et al. (2016), with local magnitudes in the range of $0 \leq M_L \leq 3.8$. Equation (6).

$$\Delta\sigma_s = \frac{C_s \mu D}{S^{1/2}}$$

By considering the static stress-drop calculated from D and the fault dimension through S and the constant C_s , it can be stated the equation (7).

$$M_0 = C_s \Delta\sigma_s S^{3/2}$$

If $M_0 = \mu DS$, then, equation (7) can be written as equation (8). $\Delta\sigma_s = 10$ -50 bar (Kanamori, 2001; Abercrombie & Leary, 1993) and C_s is considering with a value of 1 (Madariaga, 1977)

DATA & RESULTS

In order to estimate the temperature rise ΔT and the total amount of thermal energy, the seismic catalog for southern Norway for the period 2017-2018 between 3° - 12°E and 57° - 64°N has been used (<http://nnsn.geo.uib.no/nnsn/#>). For the purpose of this research, both, natural and induced seismicity are being considered (Figure 2).

The temperature increasing ΔT , calculated from equation (4) as a function of M_w is shown in Figure 3. When $w = 1$ mm and $\Delta\sigma_s = 50$ bar for $\sigma_f = 100$ bar, the maximum temperatures are observed, ranging approximately from 8°C to 140°C. The sudden heating produced during the slip by the temperature rise can cause rock weakening and thermally - related induced fracturing by decreasing friction (Byerlee, 1978). Considering the results obtained, two different phenomena could explain this behavior, which are in the following boxes.

To estimate the cumulative thermal energy produced by the events, the area was gridded using a cell size of 1.0 x 1.0 degrees. The results indicate relatively high values of thermal energy along the entire south continental margin, distributed in five well located zones marked in Figure 4.

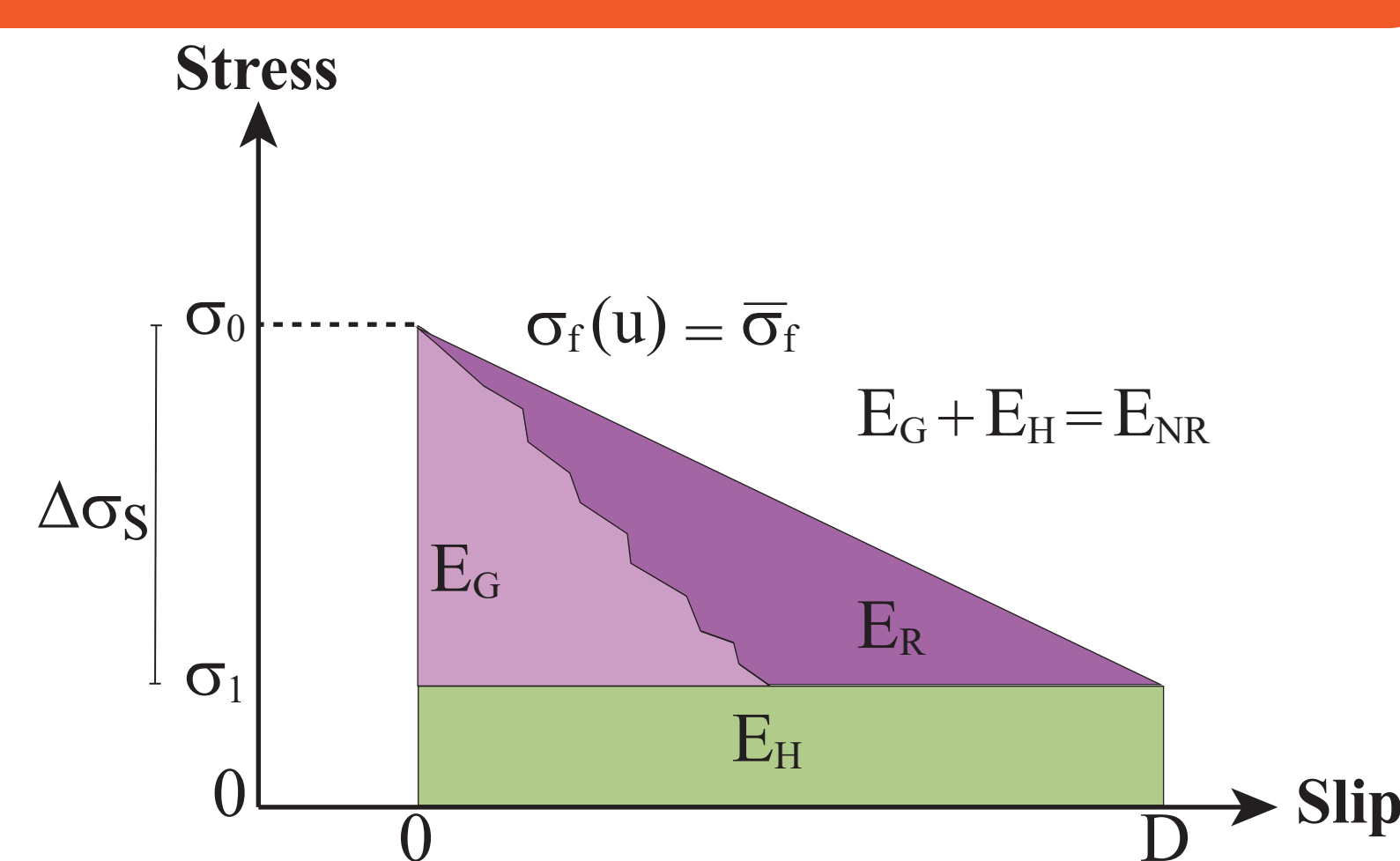


Figure 1. Schematic model of simple stress release for an earthquake. Light purple, purple and green sections correspond to the fracture, radiated and thermal energy, respectively. $\sigma_f(u)$ is defined as the average friction where u is the slip on the fault plane. Point D in the slip axis correspond to the displacement offset. Stress drop behavior can be inferred from the illustration(modified from Kanamori & Heaton, 2000)

Case 1: $\Delta T < 100^\circ\text{C}$

- Temperatures lower than 100°C are unable to trigger complex thermal processes, however, they are enough to produce volumetric thermal expansion (Robertson, 1988).
- In laboratory studies, this kind of thermal weakening constitutes an important method for inducing micro-fracturing in rock samples (Wulff & Burkhardt, 1996), mainly due to the anisotropic thermal expansion coefficients.
- Thermally induced fractures have an impact in porosity increase, decreasing or increasing of seismic velocities, pore size and local stresses (MacBeth & Schuett, 2007). This phenomenon could explain why the low-grade seismic events in southern Norway are in general distributed in well-defined weakness zones.

Case 2: $\Delta T > 100^\circ\text{C}$

- Together with mechanical effects, thermal processes become important for high magnitude earthquakes or higher temperatures.
- Regarding this, an effect of flash heating can be related with decreasing in friction in bigger earthquakes (Tisato et al., 2012; Rice, 2006).
- Depending of the permeability value, fluid pressurization can be present even with low temperature increases: less than 200°C is enough to drop the friction (Lachenbruch, 1980; Mase & Smith, 1985, 1987).
- All the events above $M_w = 3.0$ could increase the pore pressure (Figure 3).

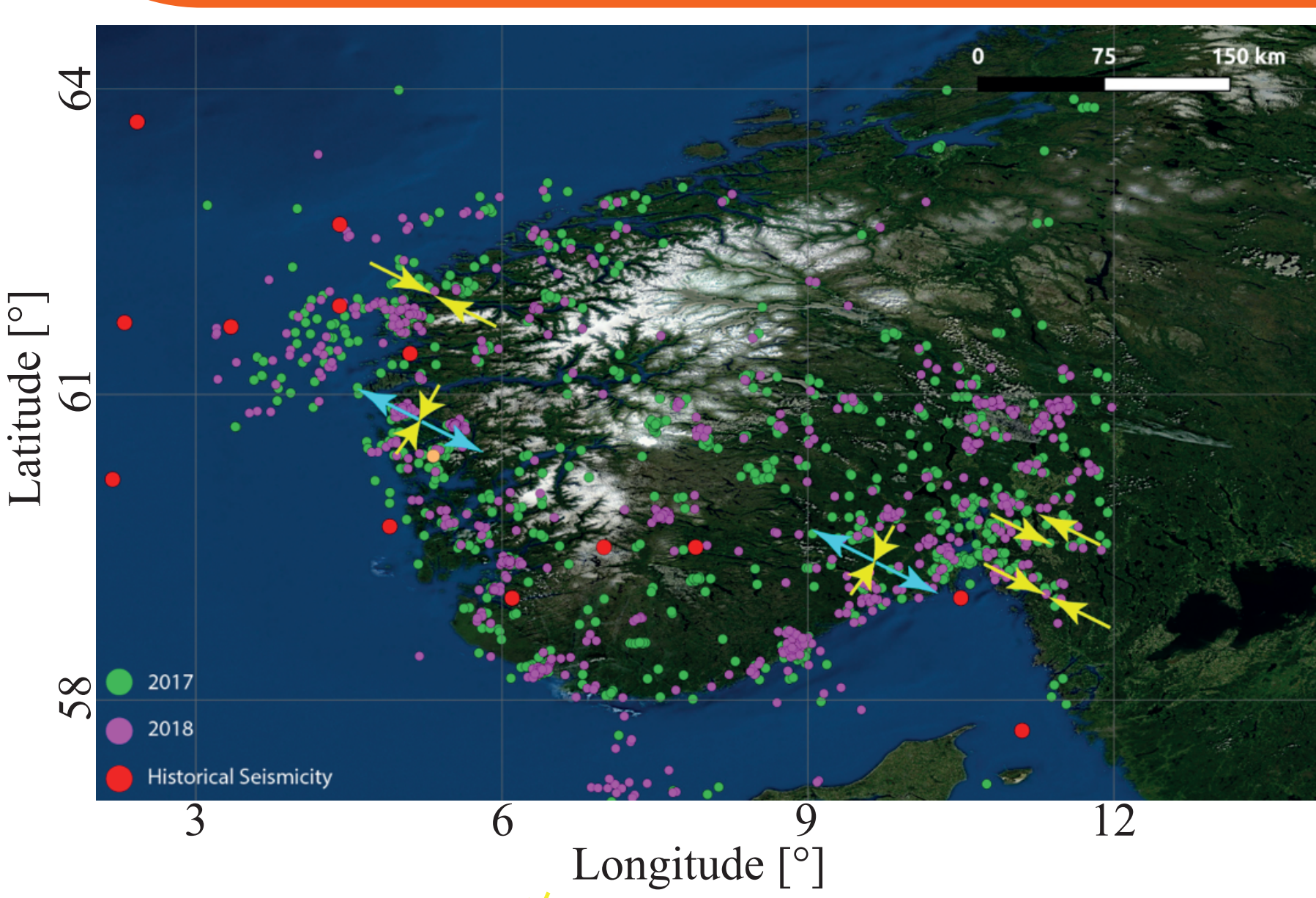


Figure 2. Seismicity in Southern Norway. Earthquakes occurring in 2017 are plotted with green circles. Purple circles are showing seismicity for 2018. Red dots correspond to 14 historical seismic events recorded in southern Norway since 1657. Yellow arrows correspond to the horizontal compression of the regional stress trends according to Fjeldskaar et al. (2000).

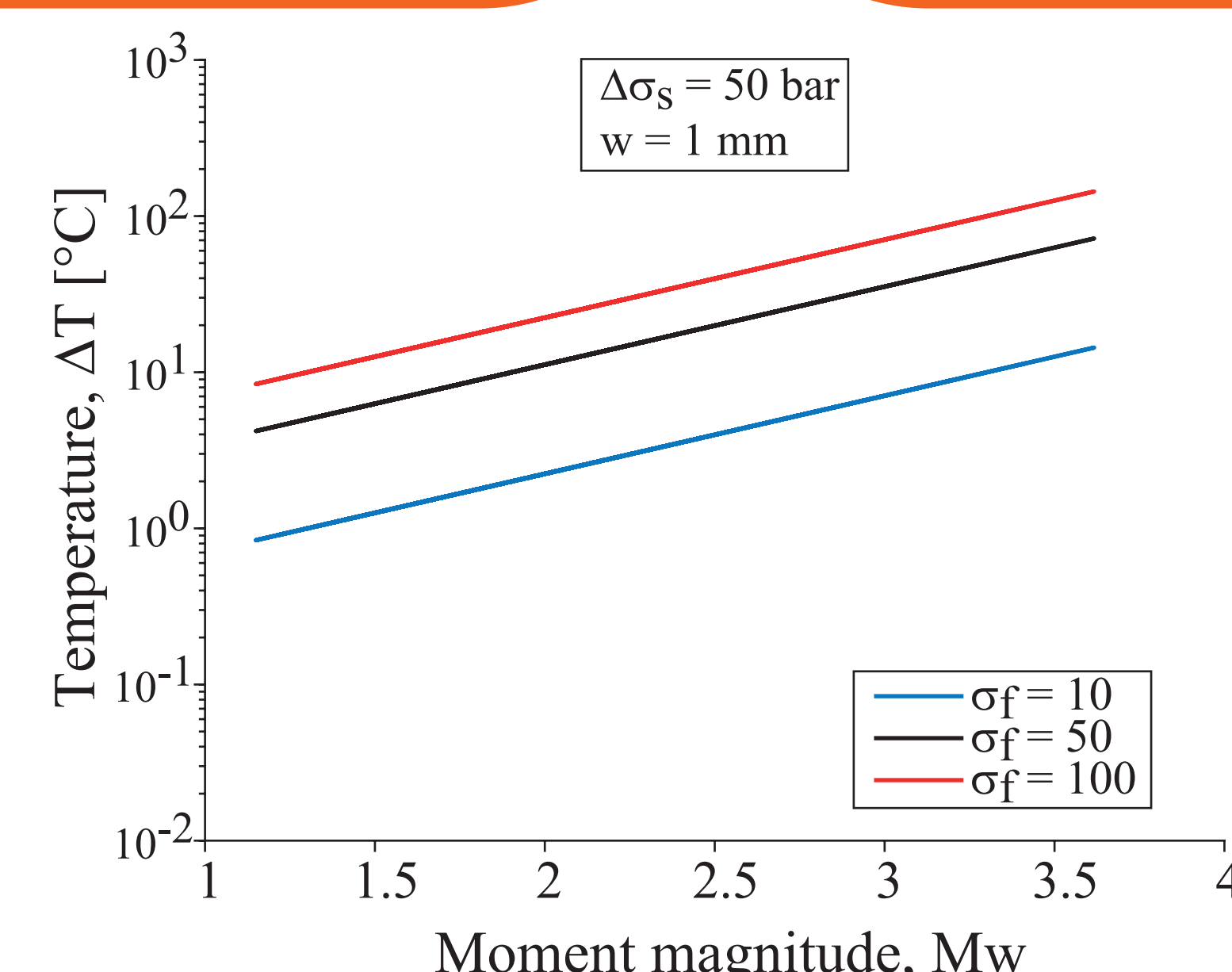


Figure 3. Temperature rise ΔT in a fault zone as function of magnitude and considering $\sigma_f = 10, 50$ and 100 bar.

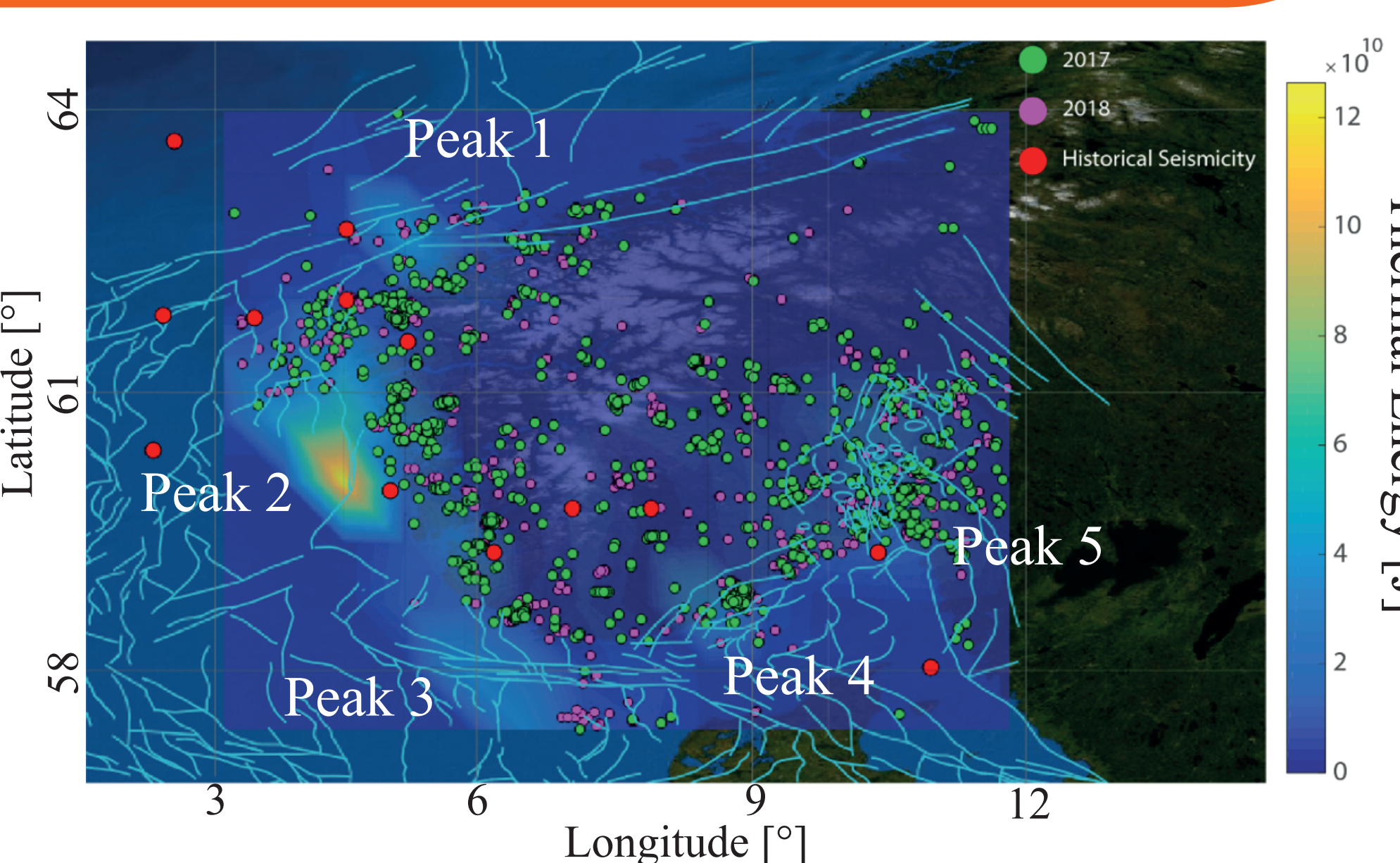


Figure 4. 2D cumulative thermal energy in southern Norway, considering $\sigma_f = 100$ bar, offshore faults (light blue lines), seismicity and historical seismicity.

Particularly, the peak 2 of thermal energy is located in the northern North Sea, south of the More basin, as is expected considering the seismicity cluster observed in the area. At the same time, peak 2 and peak 5 are clearly correlated with a high level of low grade seismicity, as well as peak 3, 4 and 5 can be related with the a high density of offshore faults. The obtained pattern by analyzing the cumulative thermal energy (Figure 4) suggested the existence of a spatial ordering in the seismicity distribution in relation with the offshore faults. Regarding this point, the Ward clustering method was applied in order to elucidate this behavior. Three well defined clusters were found (Figure 5).

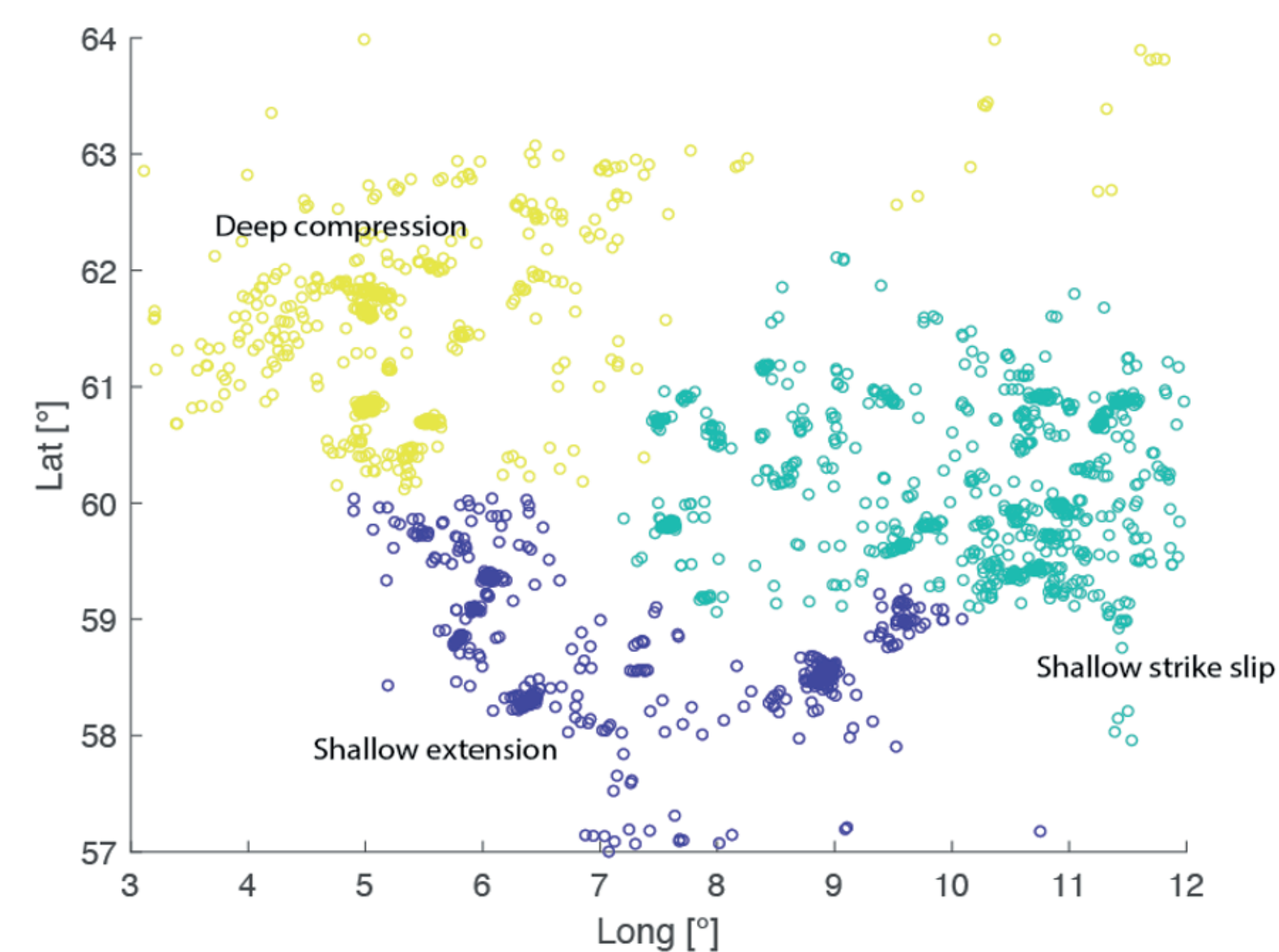


Figure 5. 2D view of the clusterization using the Ward method. The stress mechanisms are mentioned according to Fjeldskaar et al. (2000).

CONCLUSIONS

- The main weakness areas could be, among other factors, spatially limited by the heated zones related with the temperature increases due to the seismic activity, which acts as a fracturing method as well as a 'barrier', confining seismicity to remain in delineated weakness zones.
- The seismicity clusters and the thermal energy are also well correlated with the main regional stress fields (Figure 2), this may set a new approximation to the understanding of thermal energy distributions (Figure 4). This hypothesis is proposed to initiate new approaches trying to explain the nucleation of intracrustal seismicity.
- Future analysis will be done, considering a 20 years seismic catalogue. It is expected to get a better understanding of the relation between the seismic thermal budget and the regional stress in southern Norway. Also a future research will be done applying this methodology to a mining induced seismic catalogue in order to find potential industrial applications of the seismic induced energy budget.

Acknowledgements

This research is carried out with the financial support of the project "Sismicidad inducida y energía térmica: aplicación al peligro sísmico y las energías renovables" (In Spanish) founded by "Proyectos de Investigación Multidisciplinarios" by Universidad Técnica Federico Santa María, Chile (code: PI_M_19_04). CP frames this research project under the postdoctoral grant N. 74200005 "Seismic imaging using Norwegian earthquakes".

References

1. Abercrombie R. Leary P. 1993. Source parameters of small earthquakes recorded at 2.5 km depth, Cajon Pass, southern California: Implications for earthquake scaling. *Geophys. Res. Lett.* 20(14), 1511 - 1514.
2. Byerlee J. D. 1976. Friction of rocks, *Pure appl. Geophys.*, 116, 615 - 626.
3. Eshelby J. D. 1957. The determination of the elastic field of an ellipsoidal inclusion and related problems, *Proc. Royal Soc. London*, 241, 376 - 396.
4. Fjeldskaar W. Lindholm C. Dehls J. F. Fjeldskaar I. 2000. Postglacial uplift, neotectonics and seismicity in Fennoscandia, *Quaternary Science Rev.*, 19, 1413 - 1422.
5. Kanamori H. Heaton T. 2000. Microscopic and macroscopic physics of earthquakes, in *Geocomplexity and the Physics of Earthquakes*, *Geophys. Monogr. Ser.*, 120, 147 - 163, AGU, Washington, D. C..
6. Kanamori H. 2001. Chapter 11 Energy budget of earthquakes and seismic efficiency *International Geophysics*. 76: 293-305.
7. Knopoff L. 1958. Energy release in earthquakes. *Geophys. J. Int.*, 1, 44 - 52.
8. Lachenbruch A. H. 1980. Frictional heating, fluid pressure, and the resistance to fault motion, *J. Geophys. Res.*, 85, 6185 - 6222.
9. MacBeth C. Schuett H. 2007. The stress dependent elastic properties of thermally induced microfractures in aeolian Rotliegend sandstone, *Geophysical prospecting*, 55, 323 - 332.
10. Madariaga R. 1977. Implications of stress drop models of earthquakes from the inversion of stress drop from seismic observations. *Pure appl. Geophys.*, 115, 301 - 316.
11. Mase C. W. Smith L. 1985. Pore-fluid pressures and frictional heating on a fault surface, *Pure appl. Geophys.*, 122, 583 - 607.
12. Mase C. W. Smith L. 1987. Effects of frictional heating on the thermal, hydrologic and mechanical response of a fault, *J. Geophys. Res.*, 92, 6249 - 6272.
13. Munafo I. Malagnini L. Chiaraluce L. 2016. On the relationship between Mw and ML for small earthquakes, *Bull. seismo. Soc. Am.*, 106(5), 2402 - 2408.
14. Rice J. R. 2006. Heating and weakening of faults during earthquake slip, *J. Geophys. Res.*, 111(B5), 311 - 340.
15. Robertson E. 1988. Thermal properties of rocks, Open file report 88-441, United States Department of the Interior, United States Geological Survey.
16. Tisato N. Di Toro G. De Rossi N. Quaresimin M. Candela T. 2012. Experimental investigation of flash weakening in limestone, *Journal of structural geology*, 38, 183 - 199.
17. Wulff A. M. Burkhardt H. 1996. The influence of local fluid flow and microstructure on elastic and anelastic rock properties, *Surveys in Geophysics*, 17, 347 - 360.